Neuro-Oncology Advances
6(1), vdae152, 2024 | https://doi.org/10.1093/noajnl/vdae152 | Advance Access date 29 August 2024

Neuroanatomical profiles of cognitive phenotypes in patients with primary brain tumors

Jiwandeep S. Kohli, Anny Reyes, Austin Hopper, Alena Stasenko, Natalia Menendez, Kathryn R. Tringale, Mia Salans, Roshan Karunamuni, Jona A. Hattangadi-Gluth, and Carrie R. McDonald

All author affiliations are listed at the end of the article

Corresponding Author: Jiwandeep S. Kohli, PhD, Department of Psychiatry, University of California San Diego, 9452 Medical Ctr Dr, La Jolla, CA 92037, USA (jskohli@health.ucsd.edu).

Abstract

Background. Patients with brain tumors demonstrate heterogeneous patterns of cognitive impairment, likely related to multifactorial etiologies and variable tumor-specific factors. Cognitive phenotyping offers a patient-centered approach to parsing heterogeneity by classifying individuals based on patterns of impairment. The aim of this study was to investigate the neuroanatomical patterns associated with each phenotype to gain a better understanding of the mechanisms underlying impairments.

Methods. Patients with primary brain tumors were recruited for a prospective, observational study. Patients were cognitively phenotyped using latent profile analysis in a prior study, revealing 3 distinct groups: *generalized*, *isolated verbal memory*, and *minimal impairment*. Whole brain cortical thickness (CT), fractional anisotropy, and mean diffusivity (MD) were compared across phenotypes, and associations between imaging metrics and cognitive scores were explored.

Results. Neurocognitive, structural MRI, and diffusion MRI data were available for 82 participants at baseline. Compared to the minimal impairment group, the generalized impairment group showed a widespread, bi-hemispheric pattern of decreased CT (*P*-value range: .004–.049), while the verbal memory impairment group showed decreased CT (*P*-value range: .006–.049) and increased MD (*P*-value range: .015–.045) bilaterally in the temporal lobes. In the verbal memory impairment group only, increased parahippocampal MD was associated with lower verbal memory scores (*P*-values < .01).

Conclusions. Cognitive phenotypes in patients with brain tumors showed unique patterns of brain pathology, suggesting different underlying mechanisms of their impairment profiles. These distinct patterns highlight the biological relevance of our phenotyping approach and help to identify areas of structural and microstructural vulnerability that could inform treatment decisions.

Key Points

- Cognitive phenotypes in patients with primary brain tumors had unique neuroanatomical profiles
- Patients with impaired verbal memory had circumscribed temporal lobe abnormalities
- Patients with generalized impairments showed widespread cortical atrophy patterns

Importance of the Study

Neuropsychological and neuropathological heterogeneity pose significant challenges in examining specific links between brain structure and cognitive functioning in patients with brain tumors. The current study leverages cognitive phenotyping, a patient-centered approach to classifying individuals based on patterns of impairment, to better understand the neuroanatomical profiles underlying such patterns. The results highlight specific neurobiological vulnerabilities using imaging biomarkers unique to different phenotypes, as well as group-specific associations with neuropsychological performance. Examining how these phenotypes evolve over the course of treatment could be additionally helpful for understanding the effects of different interventions on cognition, and for identifying patients at risk for treatment-related decline.

Patients with primary brain tumors demonstrate heterogeneous patterns of cognitive impairment, likely related to multifactorial etiologies and variable tumor-specific factors (eg, location, size, histology, and rate of growth). This heterogeneity poses a significant challenge in examining specific links between brain structure and cognitive functioning when patients are studied as a single group. Cognitive phenotyping offers a patient-centered approach by classifying individuals based on patterns of impairment, which may lead to a more precise understanding of pathological features driving cognitive impairments in each subgroup. This approach has shown utility for determining risk for disease progression in neurological disorders such as epilepsy,[1,2] mild cognitive impairment,[3,4] and multiple sclerosis[5] but has only recently been applied to patients with primary brain tumors. In a recent study, we identified 3 unique cognitive phenotypes in patients with brain tumors, including a group with isolated memory impairment, a group with global cognitive impairment, defined as an impairment in 3 or more cognitive domains), and a minimally impaired group, characterized by no impairment in any cognitive domain.[6] Interestingly, these 3 groups did not differ in their tumor location, laterality, or size. However, the biological bases of these phenotypes have not yet been explored in terms of neuroanatomical and microstructural underpinnings.

Investigating the neuroanatomical correlates of such cognitive phenotypes in patients with brain tumors may lead to a better understanding of the mechanisms underlying different patterns of cognitive impairment while also elucidating specific risk factors for cognitive decline. Although tumor-specific factors such as location and histology can be major determinants of the onset, progression, and severity of impairment,[7–9] studies also show network disruptions[10,11] extending beyond the immediate proximity of tumors underlying cognitive changes in this population. Evidence of changes to both gray and white matter structures outside the primary tumor site supports the notion that brain tumors have the potential to cause whole-brain dysfunction and non-focal patterns of cognitive change.[12]

The current study investigated the neuroanatomical profiles that underlie cognitive phenotypes in patients with primary brain tumors before adjuvant treatment. To accomplish this goal, we examined whole-brain structural and diffusion MR imaging in a cohort of primary brain tumor patients categorized by cognitive phenotype. Cognitive phenotype groups were hypothesized to show neuroanatomical differences in line with their cognitive profiles; the isolated verbal memory group was expected to show pathological changes in medial temporal lobe regions subserving memory function while the generalized impairment group was expected to show more diffuse patterns of change. Importantly, due to the presence of cognitive and functional network dysfunction[13,14] even in patients with focal tumors, these differences were hypothesized to be only minimally influenced by specific tumor location.

Materials and Methods

Participants

Patients with primary brain tumors were recruited for an ongoing prospective, observational study examining the effects of fractionated, partial brain radiotherapy on brain microstructure and cognition between 2014 and 2023. The study was approved by the University of California, San Diego Institutional Review Board and written informed consent was obtained from all patients. Eligibility criteria included age >18 years, Karnofsky performance status >70, estimated life expectancy >1 year, and ability to undergo neurocognitive testing in English. Patients who had received prior brain radiotherapy were excluded. At the time of the current study, complete baseline neurocognitive, structural MRI, and diffusion MRI data were available for 82 participants prior to radiation treatment.

MRI Acquisition and Processing

MRI scans were collected on a 3.0T 750 GE scanner using an 8-channel head coil. Anatomical images were acquired using a 3-dimensional (3D) volumetric T1-weighted inversion recovery spoiled gradient-echo sequence (TE/TR = 2.8/6.5 ms; inversion time = 450 ms; flip angle = 8°; FOV = 24 cm). Diffusion data were acquired with a single-shot pulsed-field gradient spin EPI (echo-planar imaging) sequence (TE/TR = 96 ms/17 s; FOV = 24 cm, matrix = 128 × 128 × 48; 1.87 × 1.875 in-plane resolution; slice thickness = 2.5 mm; 48 slices) with $b = 0$, 500, 1500, and 4000 s/mm^2, with 1, 6, 6, and 15 unique gradient directions for each b-value respectively, and 1 average for each nonzero b-value. For use in nonlinear B_0 distortion correction, 2 additional $b = 0$ volumes were acquired with either forward or reverse phase-encode polarity.

Anatomical scans were processed using FreeSurfer version 5.3.0[15,16] to extract cortical thickness (CT) measurements from ROIs using the Desikan-Killiany atlas.[17] CT is calculated as the closest distance from the gray/white boundary to the gray/CSF boundary at each vertex on the tessellated surface,[18] and is often used to detect gray matter changes or cortical atrophy in both the healthy and diseased human brain. Diffusion tensors were calculated using mono-exponential fitting from $b = 0$, 500, and 1500 s/mm^2 to extract estimates of fractional anisotropy (FA) and mean diffusivity (MD). FA is a normalized measure corresponding to the degree of anisotropic diffusion, or directionality of diffusion, in a given region, often thought to reflect white matter integrity.[19] MD is an index of the molecular diffusion rate and tends to be higher in damaged tissues as a result of increased free diffusion. Diffusion tensor imaging (DTI) metrics were calculated from the co-registered DTI maps by sampling the white matter from the gray-white boundary up to 5 mm below the white matter surface normal at each vertex and then averaging within each ROI volume from the Desikan-Killiany atlas.[20,21] Tumor, surgical cavity, necrotic tissue, and regions of edema were manually censored for each patient and excluded from final ROIs prior to analysis (ie, such areas were treated as having missing data).[22,23] In terms of quality assessment procedures, the FurferSurfer surfaces were carefully examined on a slice-by-slice basis to detect any errors in the automated segmentation. The assessment was conducted independently by 2 physicians who reviewed each MRI slice by slice and subsequently reached a consensus.

Neuropsychological Data

All participants completed a comprehensive neuropsychological battery prior to radiation treatment, including measures of verbal and visual learning and memory, language, processing speed, and executive function (Table 1). Individual test scores were used for phenotyping (see Reyes et al. 2023 for detailed methods).[6] Differences in neuropsychological test scores across cognitive phenotypes are provided in Supplementary Table 1. Verbal memory was evaluated using the Hopkins Verbal Learning Test-revised,[24] resulting in Total Learning and Delayed Recall scores. A global cognitive composite score (GCC) was also calculated for each patient by averaging T-scores within and across all neuropsychological domains. HVLT-R and GCC scores were used for behavioral correlations as noted below. Quality of life was assessed with the Functional Assessment of Cancer Therapy-Brain[25] and symptoms of depression and anxiety were assessed using the Beck Depression Inventory-2[26] and Beck Anxiety Inventory, respectively.[27]

Statistical Approach

Patients were cognitively phenotyped using latent profile analysis (LPA) in a prior study (Reyes et al., in press)[6], which revealed an optimal solution of 3 distinct groups: those with generalized impairments (13.4%), those with isolated verbal memory impairments (18.3%), and those with minimal impairments (68.3%). Statistical analyses were conducted in R[28] and plots were created using the "ggplot2"[29] and "ggseg" packages.[30] Cognitive phenotypes were compared using separate ANCOVAs for CT, FA, and MD in each ROI while controlling for age, education, and sex. Follow-up pairwise comparisons were conducted for regions exhibiting significant omnibus effects with Tukey[31] adjustment for multiple comparisons. Cohen's D was calculated as an effect size estimate for significant group differences. Pearson correlations were performed to

Table 1. Neuropsychological Tests

Test	Domain	Corrections
Hopkins verbal learning test-revised (HVLT)[a]	Memory	Age
Brief visuospatial memory test (BVMT)[b]	Memory	Age
Boston naming test (BNT)[c]	Language	Age, education, sex, race
Delis-Kaplan executive function system (D-KEFS) letter fluency[d]	Language	Age
D-KEFS category fluency[d]	Language	Age
D-KEFS color-word interference test (CWIT) color naming[d]	Processing speed	Age
D-KEFS CWIT word reading[d]	Processing speed	Age
Wechsler adult intelligence scale fourth (WAIS-IV) coding subteste[e]	Processing speed	Age
D-KEFS category fluency switching accuracy[d]	Executive function	Age
D-KEFS CWIT inhibition[d]	Executive function	Age
Wisconsin card sorting test preservative errors [f]	Executive function	Age, education

[a]Benedict RH, Schretlen D, Groninger L, Brandt J. Hopkins Verbal Learning Test-Revised: Normative data and analysis of inter-form and test-retest reliability. The Clinical Neuropsychologist 1998;12:43-55.
[b]Benedict RH. Brief visuospatial memory test-revised: PAR, 1997.
[c]Kaplan E, Goodglass H, Weintraub S. Boston naming test. 2001.
[d]Delis DC, Kaplan E, Kramer JH. Delis-Kaplan executive function system. Assessment 2001.
[e]Wechsler D. Wechsler adult intelligence scale. Archives of Clinical Neuropsychology 1955.
[f]Heaton RK, Staff P. Wisconsin card sorting test: computer version 2. Odessa: Psychological Assessment Resources 1993;4:1-4.

examine the associations between neurocognitive test performance and structural and diffusion metrics in regions exhibiting significant pairwise differences. To minimize the number of statistical tests, the selection of neuropsychological measures for correlational analyses was informed by the phenotype exhibiting the significant difference in structural metrics (ie, verbal memory measures for the verbal memory impairment group and a GCC score for the generalized impairment group).

Results

Participant Characteristics

Participant characteristics of each cognitive phenotype are summarized in Table 2. Differences were observed across phenotype groups in years of education and sex. The verbal memory impairment group had fewer years of education on average compared to the minimal impairment group ($P = .063$) and a lower proportion of female patients than the other groups ($P = .004$). There were no statistically significant differences among the groups in age, race/ethnicity, history of surgery or seizures, use of antiseizure medications, or other tumor characteristics (type, grade, side, location, or IDH mutation status). Overall quality of life was significantly lower in the generalized impairment group compared to both the minimally impaired group ($P < .001$) and verbal memory impairment group ($P = .001$). The average level of depressive and anxiety-related symptoms was also higher in the generalized impairment group, though not significantly different than in the other phenotypes.

Differences in Cortical Thickness and DTI Metrics

Compared to the minimal impairment group, the generalized impairment group showed significantly lower CT in the left caudal anterior cingulate, cuneus, frontal pole, paracentral gyrus, precuneus, rostral middle frontal gyrus, superior frontal gyrus, and superior parietal lobule and right caudal middle frontal gyrus, insula, precentral gyrus, and superior parietal lobule (Figure 1A). The verbal memory impairment group showed lower CT compared to the minimal impairment group bilaterally in the entorhinal cortices and parahippocampal gyri, and in the right inferior temporal gyrus (Figure 1B). Effect sizes for all pairwise differences ranged from medium to large (Table 3).

The verbal memory impairment group additionally demonstrated higher MD compared to the minimal impairment group bilaterally in the temporal lobes, including bilateral entorhinal cortices and parahippocampal gyri, as well as in the left fusiform gyrus, inferior temporal gyrus, middle temporal gyrus, and superior temporal gyrus (Figure 2). Effect sizes for these group differences in MD also ranged from medium to large (Table 3). There were no significant differences in MD between the generalized and minimal impairment phenotypes, and there were no significant differences in FA across the groups.

Correlations With Cognitive Test Scores

Greater MD in the left parahippocampal gyrus was significantly associated with poorer HVLT Learning ($r = 0.784$; $P < .001$) and Delayed Recall ($r = 0.528$; $P < .01$) scores in the verbal memory impairment group (Figure 3). These associations were specific to the left parahippocampal region, with no significant association in the corresponding right hemisphere region. Additionally, there was no significant association between parahippocampal MD and verbal memory scores in the minimal impairment group. CT was not associated with verbal memory test scores in the verbal memory impairment group, nor with global cognitive composite scores in the generalized impairment group.

Discussion

Cognitive phenotyping offers a promising approach to understanding the heterogeneity that exists among patients with neurological disease and to studying the mechanisms and pathophysiology underlying neuropsychological dysfunction that is obscured when patients are studied in aggregate. To the best of our knowledge, only 2 studies have taken this approach to characterize cognitive impairments in adults with brain tumors. These studies identified similar neurocognitive profiles despite differences in the patient samples, including a group with learning memory impairments, a group with generalized impairment, and a group with minimal or no impairments.[32] In the current study, we build on our prior phenotyping work and identify distinct brain signatures associated with cognitive phenotypes in a cohort of patients with primary brain tumors prior to radiation treatment. The unique patterns of brain pathology identified on structural and diffusion imaging suggest different tumor and treatment-related influences related to each profile of impairment. Irrespective of tumor characteristics such as type, grade, size, and location, patients exhibiting an isolated verbal memory impairment showed neuropathological differences circumscribed to the medial and lateral temporal lobes, while those with generalized impairments showed a diffuse and bi-hemispheric pattern of cortical thinning. These results highlight the importance of taking a patient-centered approach to the study of neurotomical correlates underlying cognitive impairments in heterogeneous groups of patients, as individuals with similar profiles of impairment are likely to display similar neurobiological vulnerabilities.

Diffuse Structural Changes Related to Brain Tumors

Despite the assumption that the location of a brain tumor should be the primary driver of a patient's cognitive profile, neuroimaging studies have revealed an impact on gray matter tissue both proximal to and distant from the tumor location. For example, there has been the suggestion of homotopic reorganization characterized by increased gray matter volume in regions contralateral to brain tumors.[33] Such changes in brain structure may be related to

Table 2. Demographic and Clinical Characteristics Across Cognitive Phenotypes

	Generalized	Verbal memory	Minimal	*P*-value*
N	11	15	56	—
Percent of sample	13.4%	18.3%	68.3%	—
Age	41.64 (11.81)	43.87 (11.94)	46.43 (13.32)	.476
Education	15.20 (3.01)	13.75 (2.87)	15.98 (2.31)	.063
Sex: female	**7 (63.6%)**	**1 (6.7%)**	**28 (50.0%)**	**.004**
Race/Ethnicity				.358
White	9 (81.8%)	12 (80%)	49 (87.5%)	
African American	0 (0%)	1 (7.7%)	0 (0%)	
Asian	0 (0%)	1 (7.7%)	3 (5.4%)	
Hispanic/Latinx	2 (15.4%)	1 (7.7%)	7 (12.5%)	
Mixed	2 (15.4%)	1 (7.7%)	4 (7.1%)	
Tumor type				.181
Glioma	9 (81.8%)	10 (66.7%)	30 (53.6%)	
Other	2 (18.2%)	5 (33.3%)	26 (46.4%)	
IDH status[a]				.153
Wild-type	5 (45.5%)	4 (26.7%)	8 (14.3%)	
Mutant	4 (36.4%)	6 (40%)	22 (39.3%)	
Grade				.717
Low	3 (33.3%)	2 (20%)	10 (33.3%)	
High	6 (66.7%)	8 (80%)	20 (66.7%)	
Side				.149
Left	8 (72.7%)	9 (60%)	22 (39.3%)	
Right	2 (18.2%)	3 (20%)	26 (46.4%)	
Central	1 (9.1%)	3 (20%)	8 (14.3%)	
Location				.159
Temporal	3 (23.1%)	6 (46.2%)	9 (16.1%)	
Frontal	5 (38.5%)	4 (30.8%)	18(32.1%)	
Other	5 (38.5%)	3 (23.1%)	29 (51.8%)	
Surgery				.759
GTR/STR	9 (81.8%)	13 (86.6%)	41 (73.2%)	
Other	2 (18.1%	2 (13.3%)	15 (26.8%)	
Time between surgery and baseline testing (months)	1.0 (0.047)	.9 (0.335)	1.19 (0.496)	.393
Seizures: yes	4 (36.4%)	10 (66.7%)	25 (44.6%)	.230
ASM: yes	6 (54.5%)	11 (73.3%)	29 (51.8%)	.326
Steroid medication: yes	4 (36.4%)	8 (53.3%)	14 (25.0%)	.186
PTV	184.1 (31.6)	194.5 (49.5)	141.4 (16.9)	.317
BDI-2 total	13.00 (7.55)	7.92 (4.89)	8.33 (9.17)	.093
BAI total	12.73 (8.53)	8.49 (7.78)	5.31 (6.02)	.066
FACT-BR total	**111.63 (22.74)**	**145.03 (22.61)**	**143.81 (21.23)**	**<.001**

Abbreviations: ASM, antiseizure medications; BAI, Beck Anxiety Inventory; BDI-2, Beck Depression Inventory-2; FACT-BR, Functional Assessment of Cancer Therapy-Brain; GTR, gross total resection; PTV, planning target volume; STR, subtotal resection.
Parentheses include standard deviation or percentages.
Low: World Health Organization (WHO) grades 1 and 2; High: WHO grades 3 and 4.
Tumor Other: meningiomas, craniopharyngiomas, chondrosarcoma, pituitary adenoma, schwannoma, papillary pineal, ependymoma, germinoma.
Location Other: base of skull, cerebellar, occipital, parietal, pineal, suprasellar, thalamic.
Surgery Other: biopsy, laser interstitial thermal therapy, none.
[a]Comparisons only made for patients with gliomas.
*_P_-value corresponds to Pearson Chi-Square test or ANOVA _F_-test as appropriate; significant differences in bold.

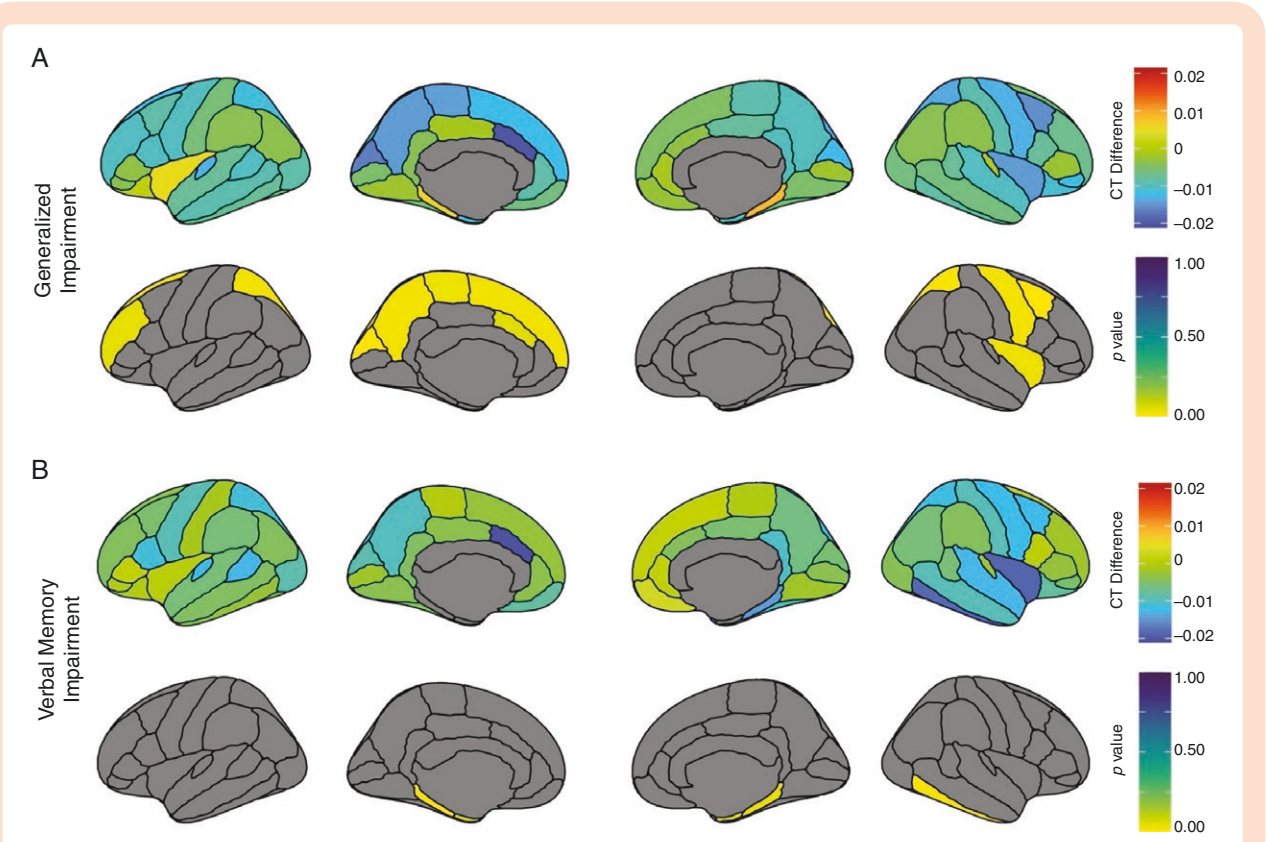

Figure 1. Cortical thickness (CT) differences are plotted across the whole brain in rows one and 3 for the generalized and verbal impairment groups respectively, compared to the minimal impairment group. Significant differences following correction for multiple comparisons are highlighted in rows 2 and 4. (A) The generalized impairment group showed significantly decreased CT compared to the minimal impairment group in the left caudal anterior cingulate ($P = .049$), cuneus ($P = .007$), frontal pole ($P = .025$), paracentral gyrus ($P = .031$), precuneus ($P = .022$), rostral middle frontal gyrus ($P = .042$), superior frontal gyrus ($P = .025$), and superior parietal lobule ($P = .022$) and right caudal middle frontal gyrus ($P = 0.004$), insula ($P = .032$), precentral gyrus ($P = .021$), and superior parietal lobule ($P = .012$). (B) The verbal memory impairment group showed decreased CT in the left entorhinal cortex ($P = .049$) and parahippocampal gyrus ($P = .015$) and right entorhinal cortex ($P = .049$), inferior temporal gyrus ($P = .043$), and parahippocampal gyrus ($P = .039$).

compensatory processes and reflect neuroplasticity,[34,35] in addition to direct disease-related changes in the areas immediately surrounding the tumor. Similarly, previous research has shown that left frontal gliomas can have global effects on cortical structure in both hemispheres, with decreases in CT and fractal dimension, a measure of topological complexity, in the contralesional hemisphere.[36] As in our study, these structural differences were notably observed irrespective of tumor volume, location, or grade. Such studies highlight the importance of considering the overall cortical networks disrupted in brain tumor patients when seeking to understand the mechanisms underlying their cognitive impairment profiles.

In addition to gray matter changes, the verbal memory impairment phenotype demonstrated higher MD of the white matter immediately underlying bilateral medial and left lateral temporal lobe regions. Higher MD is often thought of as an index of poorer white matter integrity, potentially reflecting edema or neuroinflammation.[37,38] A handful of previous diffusion MRI studies support the presence of white matter changes in regions far beyond the primary tumor and edematous regions.[39–41] Jütten et al. demonstrated decreased FA of normal-appearing white matter remote from the tumor location in glioma patients, which was associated with poorer cognitive performance.[42] Similarly, a prior study showed reduced FA within a broad structural network in glioma patients with tumor locations throughout the cerebrum. Notably, reduced FA was associated with visuospatial test impairments in a subset of patients with right temporal lobe tumors.[43] These DTI studies provide important insight into the potential mechanisms by which brain tumors impact cognitive abilities, suggesting that they are not limited to the focal region of the tumor itself. This is especially important in light of the reconceptualization of glioma and other brain tumors as a systemic rather than focal neurological disease,[44] with the potential to impact extensive cerebral networks.[45] Such results also speak to the sensitivity of diffusion MRI to microstructural changes associated with cognition in brain tumors,[20,21,23,46] as well as evidence that tissue microstructure may be more sensitive to cognitive changes than cortical thinning.[47]

Table 3. Significant Differences in Structural Metrics Compared to the Minimally Impaired Phenotype

Phenotype	Metric	Hemisphere	ROI	Mean Difference	Standard Error	*P*-value	Cohen's *d*
Generalized	CT	left	Caudal anterior cingulate	−0.201	0.084	.049	−0.709
Generalized	CT	left	Cuneus	−0.165	0.053	.007	−1.027
Generalized	CT	left	Frontal pole	−0.208	0.078	.025	−0.798
Generalized	CT	left	Paracentral	−0.142	0.055	.031	−0.814
Generalized	CT	left	Precuneus	−0.145	0.053	.022	−0.826
Generalized	CT	left	Rostral middle frontal	−0.103	0.042	.042	−0.736
Generalized	CT	left	Superior frontal	−0.123	0.046	.025	−0.797
Generalized	CT	left	Superior parietal	−0.116	0.043	.022	−0.856
Generalized	CT	right	Caudal middle frontal	−0.153	0.046	.004	−1.003
Generalized	CT	right	Insula	−0.145	0.057	.032	−0.794
Generalized	CT	right	Precentral	−0.131	0.048	.021	−0.844
Generalized	CT	right	Superior parietal	−0.136	0.046	.012	−0.866
Verbal memory	CT	left	Entorhinal	−0.370	0.155	.049	−0.651
Verbal memory	CT	left	Parahippocampal	−0.314	0.099	.006	−0.109
Verbal memory	CT	right	Entorhinal	−0.393	0.161	.043	−0.706
Verbal memory	CT	right	Inferior temporal	−0.183	0.064	.015	−0.577
Verbal memory	CT	right	Parahippocampal	−0.146	0.058	.039	−0.798
Verbal memory	MD	left	Entorhinal	2.860E-05	1.199E-05	.040	0.632
Verbal memory	MD	left	Fusiform	2.434E-05	1.024E-05	.041	0.707
Verbal memory	MD	left	Inferior temporal	2.560E-05	1.021E-05	.037	0.747
Verbal memory	MD	left	Middle temporal	2.666E-05	9.299E-06	.015	0.841
Verbal memory	MD	left	Parahippocampal	5.182E-05	1.957E-05	.026	0.402
Verbal memory	MD	left	Superior temporal	1.869E-05	7.672E-06	.045	0.717
Verbal memory	MD	right	Entorhinal	5.182E-05	1.957E-05	.026	0.851
Verbal memory	MD	right	Parahippocampal	2.860E-05	1.199E-05	.040	0.426

Abbreviations: CT, cortical thickness; MD, mean diffusivity

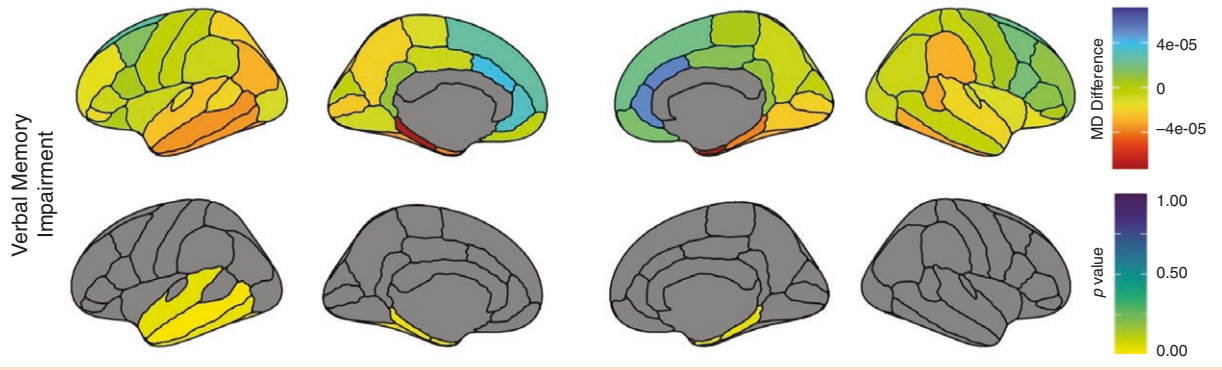

Figure 2. Mean diffusivity (MD) differences are plotted across the whole brain in row one for the verbal impairment group compared to the minimal impairment group. Significant differences following correction for multiple comparisons are highlighted in row two. There were no significant differences in MD between the generalized and verbal impairment phenotypes. The verbal memory impairment group showed significantly increased MD compared to the minimal impairment group bilaterally in the temporal lobes, including in the left entorhinal cortex ($P = .040$), fusiform gyrus ($P = .041$), inferior temporal gyrus ($P = .037$), middle temporal gyrus ($P = .015$), parahippocampal gyrus ($P = .026$), and superior temporal gyrus ($P = .045$) and right entorhinal cortex ($P = .026$) and parahippocampal gyrus ($P = .040$).

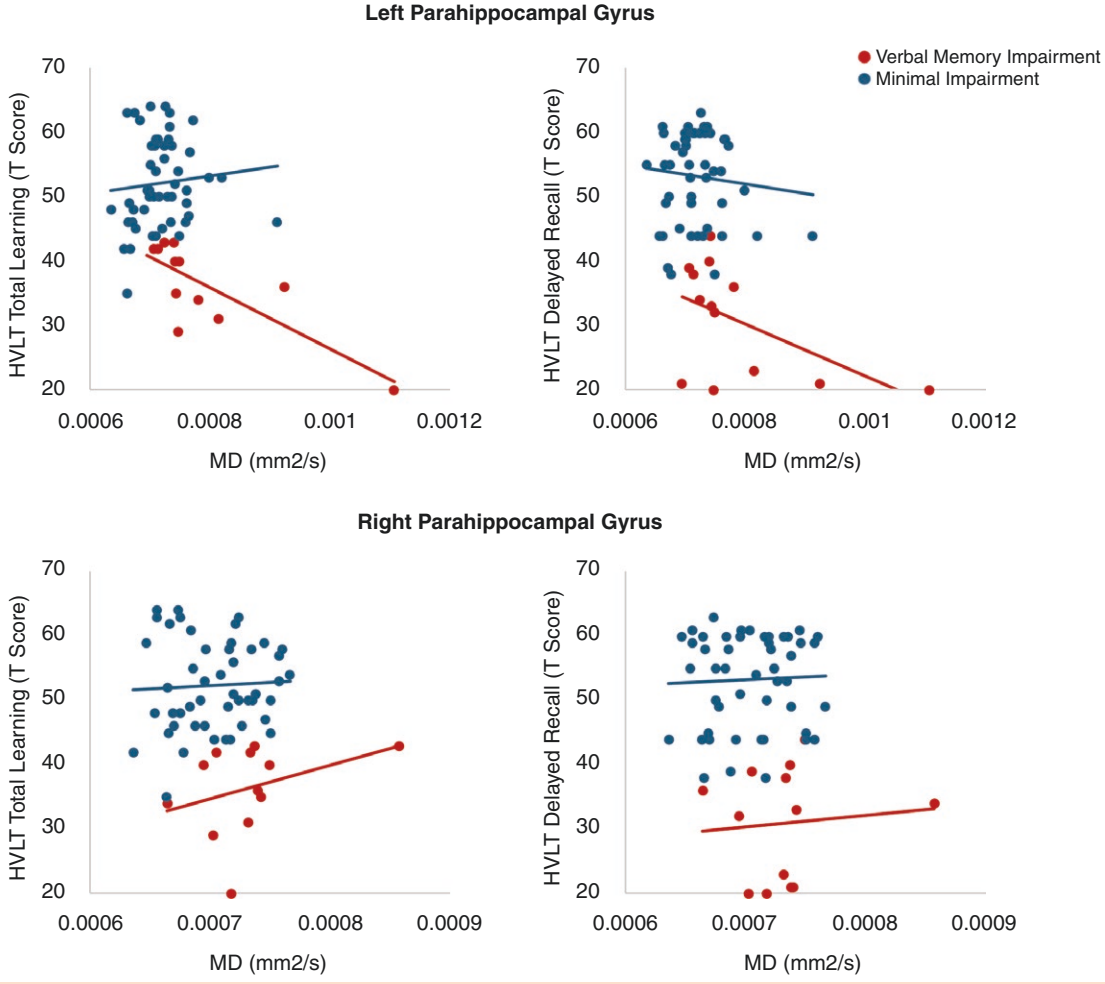

Figure 3. Greater MD in the left parahippocampal gryus was significantly associated with poorer HVLT Learning ($r = 0.784$; $P < .001$) and Delayed Recall ($r = 0.528$; $P < .01$) scores in the verbal memory impairment group, but not in the minimal impairment group. This association was not observed in the right parahippocampal gyrus.

Cognitive Phenotype-Specific Neuroanatomical Profiles

Although less than half of patients in the verbal memory impairment group had tumors located in the temporal lobes (6/13), the parahippocampal gyri and entorhinal cortices demonstrated greater structural and microstructural abnormalities compared to those with minimal cognitive impairment. Specifically, CT was reduced and MD was greater bilaterally in the parahippocampal and entorhinal regions, suggesting that local gray and white matter changes may underlie their impairment profiles. However, only higher MD in the left parahippocampal gyrus bore a significant association with impaired verbal memory, suggesting some specificity or a stronger association with this region. Notably, there was a greater proportion of male than female participants in this phenotype. This sex difference may be partially explained by a female advantage in verbal memory, with studies showing that females typically perform better in verbal memory tests than males.[48,49] In the presence of brain pathology, this advantage likely increases cognitive reserve, though the neurobiological underpinnings of this sex difference in neurocognitive performance remain to be established.

Both the parahippocampal gyrus and entorhinal cortex are involved in learning and memory, containing important efferent and afferent connections to the hippocampus.[50,51] The perforant pathway arises from this region, pathological changes to which have been implicated in Alzheimer's disease[52] and epilepsy.[53] Importantly, it has also been suggested to support other neuropsychological functions, such as visuospatial processing[54] and language.[55,56] Thus, it is unsurprising that it has been identified as playing an important role across a broad range of neurological[57–61] and psychiatric[60,62–65] conditions. Patients with brain tumors who exhibit deficits in verbal memory may therefore not only be vulnerable to additional memory decline as a result of local treatment-related effects but may also show susceptibility to changes in other cognitive domains as a result of further damage to medial temporal lobe structures and their connections. This is especially important in light of previous studies demonstrating selective vulnerability of both gray matter[66] and superficial white matter[20] in certain regions underlying higher-order cognition. Importantly, these patients demonstrated medial temporal lobe anomalies prior to the initiation of RT. Given the increased susceptibility of the temporal lobe regions to the effects of radiation,[21] the identification of such vulnerabilities could inform cognitive-tailoring interventions to prevent further cognitive decline. At the same time, it should be noted that treatment toxicities can also be diffuse, as demonstrated by a study highlighting significant treatment-associated structural brain changes following standard chemoradiation in patients with glioblastoma,[67] as well as studies of systemic treatments in other forms of cancer.[68,69] In addition to the diffuse influences of primary brain tumors themselves, such findings also have implications for the prevention of exacerbated cognitive decline in patients already demonstrating neuropsychological vulnerabilities.

The generalized impairment group showed more distributed changes than the verbal memory impairment group, with cortical thinning observed across multiple ROIs in both hemispheres, though a greater number of significant differences were observed in left hemisphere ROIs (8 out of 12). This is consistent with a greater frequency of left-sided tumors in this group (60%). This hemispheric difference is potentially meaningful in terms of the lateralization of the neuropsychological functions on which the phenotypes were based. For example, significantly lower CT in the generalized group in the left but not right caudal anterior cingulate may be related to the sensitivity of the neuropsychological tests to executive functions with more left hemisphere involvement, such as verbal fluency and switching or color-word interference. It is important to consider that the characterization of the phenotypes is based on a particular neuropsychological battery, which although comprehensive, may have led to a unique assignment of patients to groups compared to another battery, which in turn would influence the findings of specific brain regions demonstrating significant changes for each phenotype. Overall, however, the diffuse pattern of structural changes in the generalized impairment phenotype is in line with the nature of their cognitive deficits, which were global and would not necessarily be expected to correlate with anatomical changes in any one specific region of the brain. There have been several mechanisms proposed to underly such structural changes related to brain tumors during the perioperative period, including tangential stretching and compression from mass effect[70,71] and spreading of the tumor along white matter tracts leading to edema or abnormal cellularity.[72,73] Other possible mechanisms of change in CT include alterations in cell volume, dendritic shrinkage, fluctuations in astrocytic metabolic processes, or inflammatory changes.[74]

Limitations and Future Directions

The results of this study demonstrate that distinct cognitive phenotypes in patients with brain tumors have unique patterns of cortical and white matter vulnerability, revealing the biological relevance of our cognitive phenotyping approach. These findings should be interpreted in light of some limitations. Given the small sample size, larger follow-up studies will be required to expand upon these findings, particularly with regard to the regional specificity of structural changes within each phenotype. A larger sample size would also allow for the inclusion of a validation sample to confirm both the findings of the original LPA and the corresponding neuroanatomical profiles of the phenotypes. In addition, the heterogeneity in the clinical characteristics across patients may have impacted our ability to detect smaller effects. Although we may have detected the most salient regions contributing to cognitive impairments within each phenotype, other interesting associations may emerge with a larger sample size or a more homogenous sample. For the generalized impairment phenotype in particular, structural differences may be washed out at the group level due to the heterogeneity in the potential broad impacts of their tumors, which could result in impairments across multiple cognitive domains. Future studies with larger samples should further characterize the generalized impairment group, which may include subgroups of patients with different generalized profiles. It

should also be noted that cognition can be influenced by other salient factors in the brain tumor population, such as depression, anxiety, or fatigue. Although there were no significant differences among the groups on screening measures of state-dependent mood, the generalized group did show more symptoms of anxiety and depression on average, which could suggest some influence of mood on their cognitive profiles.

Relatedly, it should be noted that the average age of patients in the current study is lower than might be expected for a study of patients with primary brain tumors. Our sample included patients with brain tumors other than gliomas, with younger astrocytoma patients accounting partially for the lower average age. Additionally, patients were only enrolled in the trial if their estimated life expectancy was greater than 1 year. As such, many older patients with GBM and therefore lower estimated life expectancy were not enrolled in the study. Results may differ in an older subpopulation of patients with primary brain tumors, as older age is associated with normal declines in neurocognitive function and changes in brain anatomy, potentially leading to compounding negative effects on both.

Additionally, the current study did not include a control group of individuals without brain tumors. Rather, we leverage our minimal impairment phenotype group as a patient control group. This analytic approach offers a distinct advantage of matching across factors such as neurosurgical, seizure, and medication use history, all of which are likely to impact both cognitive function and brain structure. Due to the heterogeneity in these and other factors in our sample, we are also unable to determine to what extent brain tumors were the cause of the observed differences in neuroanatomy between phenotypes. Given the variability in both neuropsychological function and neuroanatomy in the healthy population, the associations between the structural differences and neuropsychological impairments may not be specific to patients with primary brain tumors. Future studies may also benefit from the inclusion of a healthy control group to help tease apart these considerations. This would enable us to also probe structural changes within the minimal impairment group that may serve to maintain intact cognition (eg, compensatory networks) in the presence of brain pathology. Furthermore, examination of how patterns of brain pathology within each phenotype evolve over the course of treatment could be helpful for understanding the impact of different interventions on structure-function relationships, and for identifying patients at risk for treatment-related decline.

Supplementary material

Supplementary material is available online at *Neuro-Oncology Advances* (https://academic.oup.com/noa).

Keywords:

diffusion tensor imaging | cognitive phenotypes | cortical thickness | neurocognition | neuroimaging

Funding

This work was supported by the National Institutes of Health (1KL2TR001444, UL1TR000100, and R01 CA238783-01 to J.A.H.-G; T32 MH019934 Fellowship to JK; R01 NS120976 Diversity Supplement to A.R.; 1F32NS119285-01A1 to A.S.; 1TL1TR001443 to M.S.); American Cancer Society (RSG-15-229-01-CCE to C.R.M); National Academy of Neuropsychology Clinical Research Grant (A.R.) and the Burroughs Wellcome Fund Postdoctoral Diversity Enrichment Program (A.R.).

Conflict of interest statement

The authors have no conflict of interest to disclose.

Authorship statement

J.S.K., J.H.G., and C.R.M. were involved in the design of the study; J.S.K was involved with the analysis of the data; J.S.K., A.R., J.H.G., and C.R.M. were involved with interpretation of the data; J.S.K., A.R., A.S., A.H., K.R.T., M.S., N.M., R.K., J.H.G., and C.R.M. were involved with the acquisition of the data and with the draft and review of the manuscript. All authors provided final approval of the manuscript.

Data availability

Research data are stored in an institutional repository and will be shared upon reasonable request to the senior authors.

Affiliations

Department of Psychiatry, University of California San Diego, La Jolla, California, USA (J.S.K., A.S., C.R.M.); Department of Radiation Medicine and Applied Sciences, University of California San Diego, La Jolla, California, USA (A.R., A.H., N.M., K.R.T., R.K., J.A.H.-G., C.R.M.); Department of Radiation Oncology, University of California San Francisco, San Francisco, California, USA (M.S.)

References

1. Reyes A, Kaestner E, Ferguson L, et al. Cognitive phenotypes in temporal lobe epilepsy utilizing data- and clinically driven approaches: moving toward a new taxonomy. *Epilepsia*. 2020;61(6):1211–1220.
2. Hermann B, Seidenberg M, Lee EJ, Chan F, Rutecki P. Cognitive phenotypes in temporal lobe epilepsy. *J Int Neuropsychol Soc*. 2007;13(1):12–20.

3. Bondi MW, Edmonds EC, Jak AJ, et al. Neuropsychological criteria for mild cognitive impairment improves diagnostic precision, biomarker associations, and progression rates. *J Alzheimer's Dis.* 2014;42(1):275–289.
4. Edmonds EC, Weigand AJ, Hatton SN, et al.; Alzheimer's Disease Neuroimaging Initiative. Patterns of longitudinal cortical atrophy over 3 years in empirically derived MCI subtypes. *Neurology.* 2020;94(24):e2532–e2544.
5. Hancock LM, Galioto R, Samsonov A, et al. A proposed new taxonomy of cognitive phenotypes in multiple sclerosis: the international classification of cognitive disorders in MS (IC-CoDiMS). *Mult Scler.* 2023;29(4-5):615–627.
6. Reyes A, Stasenko A, Hopper A, et al. Cognitive phenotypes: Unraveling the heterogeneity in cognitive dysfunction among patients with primary brain tumors receiving radiotherapy. *Neuro Oncol.* 2024; noae183. https://doi.org/10.1093/neuonc/noae183
7. Brown PD, Jensen AW, Felten SJ, et al. Detrimental effects of tumor progression on cognitive function of patients with high-grade glioma. *J Clin Oncol.* 2006;24(34):5427–5433.
8. Tucha O, Smely C, Preier M, Lange KW. Cognitive deficits before treatment among patients with brain tumors. *Neurosurgery.* 2000;47(2):324–333; discussion 333.
9. Zucchella C, Bartolo M, Di Lorenzo C, Villani V, Pace A. Cognitive impairment in primary brain tumors outpatients: a prospective cross-sectional survey. *J Neurooncol.* 2013;112(3):455–460.
10. Xu H, Ding S, Hu X, et al. Reduced efficiency of functional brain network underlying intellectual decline in patients with low-grade glioma. *Neurosci Lett.* 2013;543:27–31.
11. Maesawa S, Bagarinao E, Fujii M, et al. Evaluation of resting state networks in patients with gliomas: connectivity changes in the unaffected side and its relation to cognitive function. *PLoS One.* 2015;10(2):e0118072.
12. Giovagnoli AR. Investigation of cognitive impairments in people with brain tumors. *J Neurooncol.* 2012;108(2):277–283.
13. Huang Q, Zhang R, Hu X, et al. Disturbed small-world networks and neurocognitive function in frontal lobe low-grade glioma patients. *PLoS One.* 2014;9(4):e94095.
14. Stoecklein VM, Stoecklein S, Galiè F, et al. Resting-state fMRI detects alterations in whole brain connectivity related to tumor biology in glioma patients. *Neuro-Oncology.* 2020;22(9):1388–1398.
15. Dale AM, Fischl B, Sereno MI. Cortical surface-based analysis: I.Segmentation and surface reconstruction. *Neuroimage.* 1999;9(2):179–194.
16. Fischl B, Sereno MI, Dale AM. Cortical surface-based analysis: II: Inflation, flattening, and a surface-based coordinate system. *Neuroimage.* 1999;9(2):195–207.
17. Desikan RS, Ségonne F, Fischl B, et al. An automated labeling system for subdividing the human cerebral cortex on MRI scans into gyral based regions of interest. *Neuroimage.* 2006;31(3):968–980.
18. Fischl B, Dale AM. Measuring the thickness of the human cerebral cortex from magnetic resonance images. *Proc Natl Acad Sci USA.* 2000;97(20):11050–11055.
19. Soares JM, Marques P, Alves V, Sousa N. A hitchhiker's guide to diffusion tensor imaging. *Front Neurosci.* 2013;7:31.
20. Tringale KR, Nguyen T, Bahrami N, et al. Identifying early diffusion imaging biomarkers of regional white matter injury as indicators of executive function decline following brain radiotherapy: a prospective clinical trial in primary brain tumor patients. *Radiother Oncol.* 2019;132:27–33.
21. Tringale KR, Nguyen TT, Karunamuni R, et al. Quantitative imaging biomarkers of damage to critical memory regions are associated with post-radiation therapy memory performance in brain tumor patients. *Int J Rad Oncol Biol Phys.* 2019;105(4):773–783.
22. Salans M, Karunamuni R, Unnikrishnan S, et al. Microstructural cerebellar injury independently associated with processing speed in adult patients with primary brain tumors: implications for cognitive preservation. *Int J Radiat Oncol Biol Phys.* 2023;117(5):1107–1117.
23. Tibbs MD, Huynh-Le MP, Karunamuni R, et al. Microstructural injury to left-sided perisylvian white matter predicts language decline after brain radiation therapy. *Int J Radiat Oncol Biol Phys.* 2020;108(5):1218–1228.
24. Shapiro AM, Benedict RH, Schretlen D, Brandt J. Construct and concurrent validity of the Hopkins Verbal Learning Test–revised. *Clin Neuropsychol.* 1999;13(3):348–358.
25. Weitzner MA, Meyers CA, Gelke CK, et al. The Functional Assessment of Cancer Therapy (FACT) scale. Development of a brain subscale and revalidation of the general version (FACT-G) in patients with primary brain tumors. *Cancer.* 1995;75(5):1151–1161.
26. Beck AT, Steer RA, Brown GK. *Beck Depression Inventory.* San Antonio, TX. 1987.
27. Beck AT, Steer R. *Beck Anxiety Inventory Manual.* San Antonio, TX. 1993.
28. R Core Team. *R: A Language and Environment for Statistical Computing.* 2020. https://www.R-project.org/. Accessed May 13, 2024.
29. Wickham H. *ggplot2: Elegant graphics for data analysis.* 2016. https://ggplot2.tidyverse.org. Accessed May 13, 2024.
30. Mowinckel AM, Vidal-Piñeiro D. *Visualisation of Brain Statistics With R-Packages ggseg and ggseg3d.* 2019. https://github.com/ggseg. Accessed May 13, 2024.
31. Tukey JW. The philosophy of multiple comparisons. *Stat Sci.* 1991;6(1)::100–116.
32. Röttgering JG, Taylor JW, Brie M, et al. Understanding the association between fatigue and neurocognitive functioning in patients with glioma: a cross-sectional multinational study. *Neurooncol Pract.* 2024;11(3):284–295.
33. Almairac F, Duffau H, Herbet G. Contralesional macrostructural plasticity of the insular cortex in patients with glioma: a VBM study. *Neurology.* 2018;91(20):e1902–e1908.
34. Lv K, Cao X, Wang R, et al. Neuroplasticity of glioma patients: brain structure and topological network. *Front Neurol.* 2022;13:1–13.
35. Mitolo M, Zoli M, Testa C, et al. Neuroplasticity mechanisms in frontal brain gliomas: a preliminary study. *Front Neurol.* 2022;13:867048.
36. Kinno R, Muragaki Y, Maruyama T, et al. Differential effects of a left frontal glioma on the cortical thickness and complexity of both hemispheres. *Cereb Cortex Commun.* 2020;1(1):tgaa027.
37. Alexander AL, Lee JE, Lazar M, Field AS. Diffusion tensor imaging of the brain. *Neurotherapeutics.* 2007;4(3):316–329.
38. Avram AV, Sarlls JE, Basser PJ. Measuring non-parametric distributions of intravoxel mean diffusivities using a clinical MRI scanner. *Neuroimage.* 2019;185:255–262.
39. Price SJ, Burnet NG, Donovan T, et al. Diffusion tensor imaging of brain tumours at 3 T: a potential tool for assessing white matter tract invasion? *Clin Radiol.* 2003;58(6):455–462.
40. Kallenberg K, Goldmann T, Menke J, et al. Glioma infiltration of the corpus callosum: early signs detected by DTI. *J Neurooncol.* 2013;112(2):217–222.
41. Won YI, Chung CK, Kim CH, et al. White matter change revealed by diffusion tensor imaging in gliomas. *Brain Tumor Res Treat.* 2016;4(2):100–106.
42. Jütten K, Mainz V, Gauggel S, et al. Diffusion tensor imaging reveals microstructural heterogeneity of normal-appearing white matter and related cognitive dysfunction in glioma patients. *Front Oncol.* 2019;9:536.
43. Liu D, Liu Y, Hu X, et al. Alterations of white matter integrity associated with cognitive deficits in patients with glioma. *Brain Behav.* 2020;10(7):e01639.
44. Sahm F, Capper D, Jeibmann A, et al. Addressing diffuse glioma as a systemic brain disease with single-cell analysis. *Arch Neurol.* 2012;69(4):523–526.

45. Osswald M, Jung E, Sahm F, et al. Brain tumour cells interconnect to a functional and resistant network. *Nature.* 2015;528(7580):93–98.
46. Makale MT, McDonald CR, Hattangadi-Gluth JA, Kesari S. Mechanisms of radiotherapy-associated cognitive disability in patients with brain tumours. *Nat Rev Neurol.* 2017;13(1):52–64.
47. Ziegler DA, Piguet O, Salat DH, et al. Cognition in healthy aging is related to regional white matter integrity, but not cortical thickness. *Neurobiol Aging.* 2010;31(11):1912–1926.
48. Voyer D, Saint Aubin J, Altman K, Gallant G. Sex differences in verbal working memory: a systematic review and meta-analysis. *Psychol Bull.* 2021;147(4):352–398.
49. Sundermann EE, Maki PM, Rubin LH, et al.; Alzheimer's Disease Neuroimaging Initiative. Female advantage in verbal memory. *Neurology.* 2016;87(18):1916–1924.
50. Witter MP, Wouterlood FG, Naber PA, Van Haeften T. Anatomical organization of the parahippocampal-hippocampal network. *Ann N Y Acad Sci.* 2000;911(1):1–24.
51. Hoesen GWV. The parahippocampal gyrus: New observations regarding its cortical connections in the monkey. *Trends Neurosci.* 1982;5:345–350.
52. Hyman BT, Van Hoesen GW, Kromer LJ, Damasio AR. Perforant pathway changes and the memory impairment of Alzheimer's disease. *Ann Neurol.* 1986;20(4):472–481.
53. Loi RQ, Leyden KM, Balachandra A, et al. Restriction spectrum imaging reveals decreased neurite density in patients with temporal lobe epilepsy. *Epilepsia.* 2016;57(11):1897–1906.
54. Kravitz DJ, Saleem KS, Baker CI, Mishkin M. A new neural framework for visuospatial processing. *Nat Rev Neurosci.* 2011;12(4):217–230.
55. Lin YH, Dhanaraj V, Mackenzie AE, et al. Anatomy and white matter connections of the parahippocampal gyrus. *World Neurosurgery.* 2021;148:e218–e226.
56. Sharp DJ, Scott SK, Wise RJ. Retrieving meaning after temporal lobe infarction: the role of the basal language area. *Ann Neurol.* 2004;56(6):836–846.
57. Köhler S, Black SE, Sinden M, et al. Memory impairments associated with hippocampal versus parahippocampal-gyrus atrophy: an MR volumetry study in Alzheimer's disease. *Neuropsychologia.* 1998;36(9):901–914.
58. Chen G, Ward BD, Chen G, Li SJ. Decreased effective connectivity from cortices to the right parahippocampal gyrus in Alzheimer's disease subjects. *Brain Connect.* 2014;4(9):702–708.
59. Guedj E, Bettus G, Barbeau EJ, et al. Hyperactivation of parahippocampal region and fusiform gyrus associated with successful encoding in medial temporal lobe epilepsy. *Epilepsia.* 2011;52(6):1100–1109.
60. Razi K, Greene KP, Sakuma M, et al. Reduction of the parahippocampal gyrus and the hippocampus in patients with chronic schizophrenia. *Br J Psychiatry.* 1999;174(6):512–519.
61. Pillay N, Fabinyi GC, Myles TS, et al. Parahippocampal epilepsy with subtle dysplasia: a cause of "imaging negative" partial epilepsy. *Epilepsia.* 2009;50(12):2611–2618.
62. Escartí MJ, de la Iglesia-Vayá M, Martí-Bonmatí L, et al. Increased amygdala and parahippocampal gyrus activation in schizophrenic patients with auditory hallucinations: an fMRI study using independent component analysis. *Schizophr Res.* 2010;117(1):31–41.
63. Takahashi T, Suzuki M, Zhou SY, et al. Temporal lobe gray matter in schizophrenia spectrum: a volumetric MRI study of the fusiform gyrus, parahippocampal gyrus, and middle and inferior temporal gyri. *Schizophr Res.* 2006;87(1):116–126.
64. Zamoscik V, Huffziger S, Ebner-Priemer U, Kuehner C, Kirsch P. Increased involvement of the parahippocampal gyri in a sad mood predicts future depressive symptoms. *Soc Cogn Affect Neurosci.* 2014;9(12):2034–2040.
65. Almeida JRC, Mechelli A, Hassel S, et al. Abnormally increased effective connectivity between parahippocampal gyrus and ventromedial prefrontal regions during emotion labeling in bipolar disorder. *Psychiatry Res.* 2009;174(3):195–201.
66. Seibert TM, Karunamuni R, Kaifi S, et al. Cerebral cortex regions selectively vulnerable to radiation dose-dependent atrophy. *Int J Rad Oncol Biol Phys.* 2017;97(5):910–918.
67. Prust MJ, Jafari-Khouzani K, Kalpathy-Cramer J, et al. Standard chemoradiation for glioblastoma results in progressive brain volume loss. *Neurology.* 2015;85(8):683–691.
68. Henneghan A, Rao V, Harrison RA, et al. Cortical brain age from pretreatment to post-chemotherapy in patients with breast cancer. *Neurotox Res.* 2020;37(4):788–799.
69. Deprez S, Amant F, Yigit R, et al. Chemotherapy-induced structural changes in cerebral white matter and its correlation with impaired cognitive functioning in breast cancer patients. *Hum Brain Mapp.* 2011;32(3):480–493.
70. Hogea C, Davatzikos C, Biros G. Modeling glioma growth and mass effect in 3D MR images of the brain. In: *International Conference on Medical Image Computing and Computer-Assisted Intervention.* Berlin, Heidelberg, Germany: Springer; 2007:642–650.
71. Miller P, Coope D, Thompson G, Jackson A, Herholz K. Quantitative evaluation of white matter tract DTI parameter changes in gliomas using nonlinear registration. *Neuroimage.* 2012;60(4):2309–2315.
72. Engwer C, Hillen T, Knappitsch M, Surulescu C. Glioma follow white matter tracts: a multiscale DTI-based model. *J Math Biol.* 2015;71(3):551–582.
73. Wang J, Yi L, Kang Q, et al. Glioma invasion along white matter tracts: a dilemma for neurosurgeons. *Cancer Lett.* 2022;526:103–111.
74. Vidal-Pineiro D, Parker N, Shin J, et al.; Alzheimer's Disease Neuroimaging Initiative and the Australian Imaging Biomarkers and Lifestyle Flagship Study of Ageing. Cellular correlates of cortical thinning throughout the lifespan. *Sci Rep.* 2020;10(1):21803.